Geospatial Health 8(2), 2014, pp. 353-364

Study of the variation of schistosomiasis risk in Lake Poyang in the People's Republic of China using multiple space-borne sensors for monitoring and modelling

Kuo-Hsin Tseng[1,2], Song Liang[3], Motomu Ibaraki[1], Hyongki Lee[4], C. K. Shum[1,5]

[1]Division of Geodetic Science, School of Earth Sciences, The Ohio State University, Ohio, USA; [2]College of Public Health, The Ohio State University, Ohio, USA; [3]Department of Environmental and Global Health, University of Florida, Florida, USA; [4]Department of Civil and Environmental Engineering, University of Houston, Texas, USA; [5]Insitute of Geodesy and Geophysics, Chinese Academy of Sciences, Wuhan, China

Abstract. The dynamics of the Poyang Lake in Jiangxi province, People's Republic of China has been monitored to demonstrate the association of various variables with the distribution of schistosomiasis transmission with particular reference to the annual variation of the habitats for the *Oncomelania* snail, the intermediate host of *Schistosoma japonicum*. This was studied with multiple space-borne sensors, including the ENVISAT radar altimeter (RA-2) and MODIS/Terra radiometry data products such as the 16-day enhanced vegetation index, the 8-day sun reflectance, and the derived modified normalized difference water index. The measurements of physical properties were in good accordance with previous reports based on *in situ* gauge data, spectroradiometry and other optical methods, which encouraged us to build a predictive model based on reported geospatial constraints to assess the limits of potential variation of the snail habitat areas. The simulated results correspond fairly well with surveys conducted by local authorities showing a correlation coefficient of 0.82 between high-potential habitat areas and local estimates in a 9-year (2002-2010) analysis. Taken together, these data indicate that space-borne observations and *in situ* measurements can be integrated and used as a first step of a monitoring system for control and analysis of the potential of schistosomiasis dissemination. Since the true range and intensity of transmission in the study region remain elusive at present, a long-term survey around the lake is warranted to build a robust, parametric model.

Keywords: ENVISAT altimetry, MODIS, remote sensing, schistosomiasis, infectious disease, People's Republic of China.

Introduction

In the People's Republic of China (P.R. China), control of schistosomiasis has reduced the number of infected people from over 11 million in the 1950s to approximately one million in 1995 (Utroska et al., 1989; Utzinger et al., 2005; Wu et al., 2005). The number has been further reduced reaching ~326,000 in 2010 and 289,000 in 2011 (Lei et al., 2011; Chen, 2014). However, a remarkable re-emergence of schistosomiasis took place between 1995 and 2005. The number of patients with acute disease in certain villages bounced back 37% in the first 5 years (1995-2000) (Liang et al., 2007) and an additional 16% increase occurred thereafter (Wu et al., 2005; Zhou et al., 2005). The re-emergence of schistosomiasis, especially along the mid-tier of the Yangtze River basin and the Dongting and Poyang lakes (Fig. 1), is arguably due to large-scale, anthropogenic environmental transformation and regional climate change (Li et al., 2007) but also the result of specific policies administered in response to the massive flooding event of 1998 (Duan and Steil, 2003). These factors increased suitable snail habitats and led to higher transmission. Two mandatory policies termed "Return reclaimed farmland to the lake" and "Direct flooding to the plains via embankment construction", might have promoted the spread of snails across well-established dyke systems once recognised as an effective barrier (Chen and Lin, 2004). The third land policy "Build new township for relocated residents" resulted in the transfer of people from flooded areas upstream near the construction of the Three Gorges Dam in the Yangtze River to lowland areas far away from the dam. This resulted in the movement of more than two million people, as well as cattle, in the early 2000s from non-endemic areas to new habitations, some of them in endemic areas (Ross et al., 2001; Li et al., 2007).

Corresponding author:
Kuo-Hsin Tseng
Division of Geodetic Science, School of Earth Sciences
Ohio State University
275 Mendenhall Lab, 125 S Oval Mall, Columbus, OH 43210, USA
Tel. +1 61 4886-8168; Fax +1 61 4292-7688
E-mail: tseng.95@osu.edu

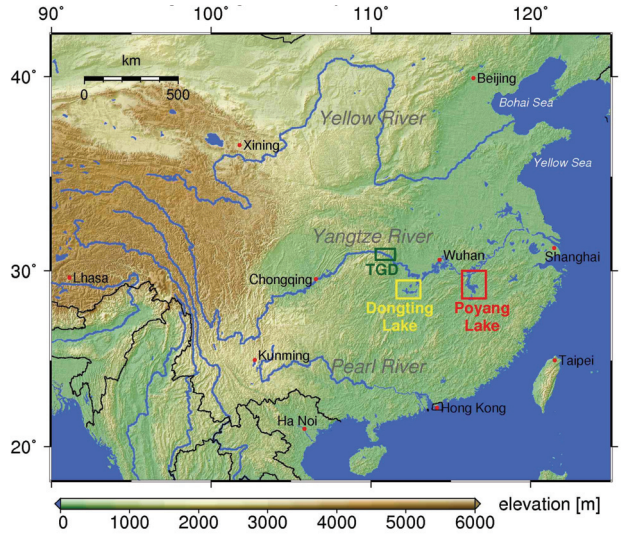

Fig. 1. Geographical locations of the Poyang Lake (red), the Dongting Lake (yellow), the Three Gorges Dam (green) and major rivers in P.R. China. Topography colour-coded by GTOPO30 digital elevation model (DEM).

Schistosomiasis-endemic areas are found almost along the entire Yangtze River basin from Yunnan and Sichuan provinces upstream to Anhui and Jiangsu provinces downstream (Spear et al., 2002; Zhou et al., 2007). Spear et al. (2004) surveyed infection prevalence at the Qionghai Lake in south-western Sichuan province showing that farmers constituted approximately 30% of all infected cases, primarily due to use of untreated manure fertiliser and irrigation systems that exchanged contaminated water between farming areas, villages and lakes. Accordingly, water dynamics, including overflow along waterways, channels, crop fields and sewage works dominate seasonal snail reproduction and can hence be referred as the pathway of disease transmission.

The amphibious *Oncomelania hupensis* snail, the intermediate host of *Schistosoma japonicum*, emerges during March to April after winter hibernation and starts to produce eggs. Newborn snails appear in late spring just before the first flood of the Yangtze River resulting in the first sub-peak of schistosomiasis prevalence of the year ahead of the major peak in September-November. In early June, aquatic, immature snails are spread widely as flooding immerses most of the floodplains. The extent of potential snail habitats is determined during the wet season and depends on the expanse of inundated areas. After the water recedes in September, massive numbers of adult snails inhabit the agricultural fields and the green marsh grounds that people and grasing cattle frequently visit and thereby close the parasite lifecycle accelerating spread of the disease. The uniqueness of these water dynamics in Poyang Lake results in peak schistosomiasis transmission between September and November (McManus et al., 2010).

Advances in satellite-borne observation offer the opportunity for continuous monitoring of the environmental factors at the scale of the lake basin, while avoiding spatial limitations (due to difficult terrestrial access) in traditional surveying techniques (Alsdorf et al., 2007). Active remote-sensing or geodetic sensors including satellite altimetry, global positioning systems (GPS), interferometric synthetic aperture radar (InSAR), as well as infrared/passive-microwave sensors, i.e. the Moderate Resolution Imaging Spectroradiometer (MODIS), the Advanced Very High Resolution Radiometer (AVHRR) and the Advanced Microwave Scanning Radiometer for EOS (AMSR-E) have been innovatively used as monitoring tools for providing data from water bodies, where *in situ* gauge data are insufficient for hydrologic studies (Kim et al., 2009; Westra and De Wulf, 2009; Zhang et al., 2010; Jung et al., 2011; Lee et al., 2011). The MODIS instrument onboard NASA's Terra and Aqua satellites is particularly useful for the studies embarked on here, as it not only monitors the atmospheric composition and thermal variation (Tseng et al., 2011), but also surveys estuarine water colour and ecosystems thanks to its multi-bands proportional indices (Hu et al., 2004). During the past three decades, more than 30 altimeters or remote-sensing instruments have thus been operated onboard satellites or used in space shuttle studies.

Launched in March 2002, the European Space Agency (ESA)'s environmental satellite (ENVISAT) follows the European remote-sensing satellite (ERS) two missions to synoptically study ocean, ice-sheet, land cover and hydrologic basins with a suite of geodetic and remote-sensing instruments, including a dual-frequency radar altimeter. The approximately two-decade time series constructed by ERS-1 and ERS-2 and the ENVISAT satellite altimetry measurements not only facilitate studies of medium-scale ocean dynamics such as tides, ocean circulation, and secular sea level changes (Fu and Cazenave, 2001), but can also be utilised for other geophysical applications, e.g. monitoring vertical motion of land, inland hydrology, sea-ice and ice-sheet elevation changes (Lee et al., 2013; Tseng et al., 2013). Payloads onboard ENVISAT can be integrated with other optical devices to study floods and drought related to river basins (Lu et al., 2009). Uribe et al. (2009) demonstrated the synergy of the Advanced-SAR (ASAR) and the Medium-

spectral Resolution Imaging Spectrometer (MERIS) onboard ENVISAT to monitor floodplains within the Dongting and Poyang lakes, where the inundated area delineation meshes well with another optical high-resolution Beijing-1 microsatellite data (Wang et al., 2007).

Integrated geospatial approaches, including geographical information systems (GIS) and remote sensing, have been widely used for monitoring, modelling and cluster analysis in P.R. China (Davis et al., 2002; Zhang et al., 2009; McManus et al., 2010; Peng et al., 2010). However, characterising water dynamics and the mechanisms underlying water-borne diseases is still a challenge, in part due to limitation in obtaining accurate information about land use (e.g. the various agricultural types) and human activities (e.g. farming and grasing cattle). In this light, it is obvious that the key to prevention of schistosomiasis lies in better understanding of snail population dynamics and snail habitats. Since our knowledge of the range and intensity of schistosomiasis around the Poyang Lake (as well as other lakes and waterways) is far from complete, a long-term survey of the lake is warranted to collect the data needed to build a robust, parametric model of how a barrier between disease and the seasonal variations of the water level can be erected.

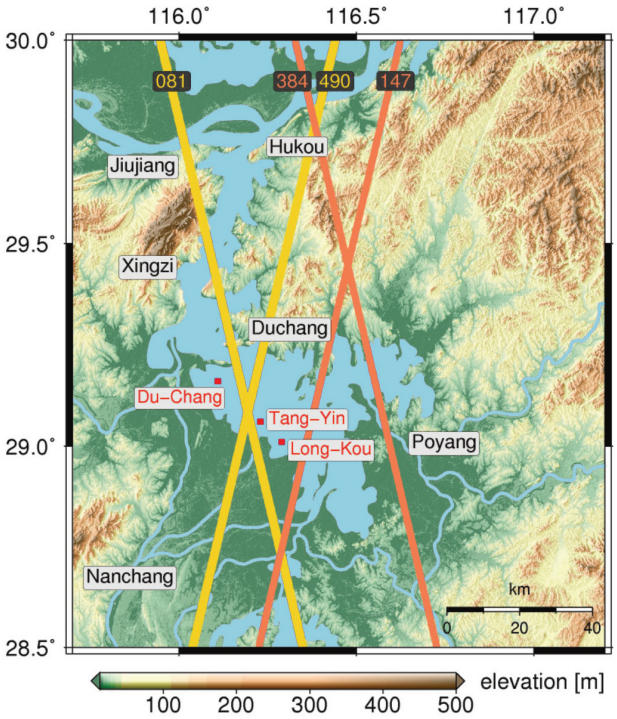

Fig. 2. The Poyang Lake area with the three water level gauges (red text) showing the long-term average water surface with the Yangtze River passing the northern inlet. Background topography with colour-coded elevations according to the SRTM3 DEM. The crossing lines are two sets of ENVISAT ground tracks before (yellow) and after (orange) the orbit change in 2010. The water boundary refers to the World Vector Shorelines (WVS) and CIA World Data Bank II (WDBII) composed by the Generic Mapping Tools (GMT) (Wessel and Smith, 2010).

Materials and methods

Study site

The Poyang Lake, located approximately at latitude 29.2° N and longitude 116.2° E in the northern part of Jiangxi province, is the largest water body in P.R. China (Fig. 1). Records covering 1956-2005 indicate the average level of the lake at the Hukou gauge station (29.74° N, 116.21° E, north of the basin) as varying annually between 8.15-17.75 m above the mean sea level (MSL) (Liu, 2006). This corresponds to a water surface change of 1,000 to 3,500 km^2 (Qi et al., 2009), which provides an excellent environment for the *Oncomelania* snail as described by Chen and Lin (2004).

Fig. 2 shows the ENVISAT satellite ground tracks overlaying the Poyang Lake before and after its orbit change in 2010. The yellow lines outline the ground tracks before the orbit change (the period 2002-2010) with a 35-day repeat cycle and a resolution of approximately 80 km (between paralleled tracks at the equator), while the orange lines show the later 30-day repeating tracks with a somewhat coarser ground resolution of ~93 km. The computation of the water level before the orbit change included passages #081 and #490. Both time series were later connected to #147 measurements with a gradient correction of the topographic difference. Passage #384 after the orbit change only covered a limited water area and was therefore omitted. Data from the three major water level gauges within the lake area, Du-Chang, Tang-Yin and Long-Kou, were obtained between the end of 2002 and 2005. This 3-year ground observation was used to validate the ENVISAT radar altimetry observations for cycles 10-42.

Remote sensing by space-borne observers

ENVISAT altimetry data were used since they had been evaluated in this region (Chu et al., 2008) to adjust the threshold for computing the MODIS water index. The latter was used to demonstrate the accuracy of the water profiles in comparison with the results reported by Uribe et al. (2009). Since the intermittent submergence around the Poyang Lake has both temporally and spatially irregular distributions (Uribe et

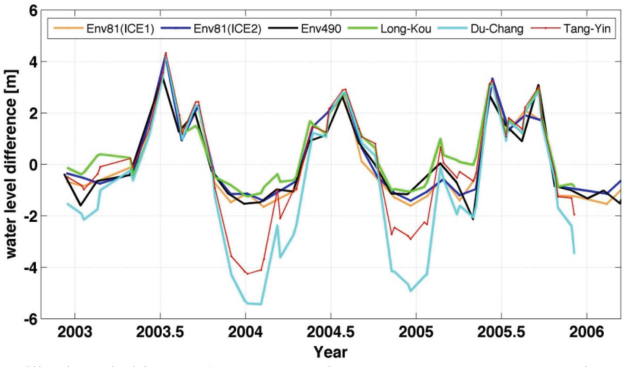

Fig. 3a. The Poyang Lake water level variation between 2003 and 2006 estimated by ENVISAT altimetry and *in situ* gauges. Three-way satellite-based altimetry (ICE-1 re-tracker at pass #81, ICE-2 re-tracker at pass #81 and ICE-2 re-tracker at pass #490) compared with three fixed *in situ* gauges at Long-Kou, Du-Chang and Tang-Yin.

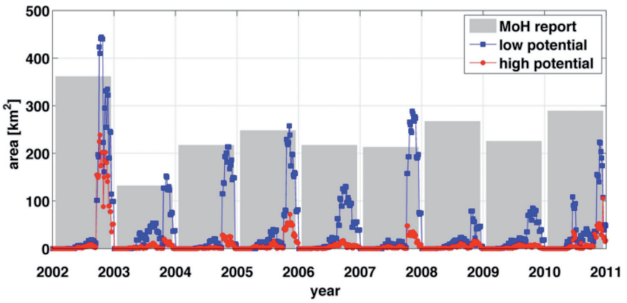

Fig. 3b. The Poyang Lake water level variation between 2003 and 2011 estimated by ENVISAT altimetry and water surface by MODIS between 2000 and 2011. Satellite-based altimetry at ENVISAT passes #81 and #490 (left ordinate, measuring lake level) compared with seasonal changes in water surface obtained from MODIS (right ordinate, measuring lake area).

al., 2009) and the on-site gauge data only provide partial measurements over the entire floodplain, multiple data sources are required to complete the water coverage estimate (Fig. 3). In this study, we used two cloud-free imagery series from MODIS/Terra: the 8-day sun reflectance (SR) (MOD09A1) and the 16-day enhanced vegetation index (EVI) (MOD13A1) to estimate the seasonal change of the water surface and canopy structure in the Poyang Lake. We further consolidated all these parameters and used reported, geospatial constraints (Chen and Lin, 2004; Zhang et al., 2009) to estimate potential maximum and minimum snail habitat areas.

Space-borne water data and processing methods

Altimetry and Radiometry

The basic concept of satellite altimetry is to measure the two-way travel time of radar impulses emitted and received by a dual-frequency radar altimeter. One half of the time difference between the signal radiated from onboard altimeter and the reception of reflected signal from nadir topographic surface is then converted into an initial, tele-metered range. Instrumental and environmental corrections are required for each measurement since the medium between space-borne radar altimeter and the surface is non-homogeneous, which can substantively advance or delay the transmitted signals (Lee et al., 2010). Instrumental corrections include Doppler shift and oscillator drift. Other media and geophysical corrections include ionosphere, dry/wet troposphere, solid Earth tide and pole tide. Subsequent to media corrections applied to the initial distance, radar waveform re-tracking is another important correction used for fine-tuning height estimates for certain type of topographic surfaces (Tseng et al., 2014). Waveform re-tracking algorithms are accordingly designated for matching typical patterns of waveform returned from ice, ocean, land, etc. For example, the ocean re-tracker (Brown, 1977) normally fits the waveform shape with a steep leading edge and a gradual descent in the tail, while the ICE re-trackers (Davis, 1997) fit the multi-peaks pattern in the waveform, whose pulse-limited footprint contains various strength of specular reflection. Although four default re-trackers: ICE-1, ICE-2, SEAICE and OCEAN archived in ENVISAT geophysical data record (GDR) are originated for oceanographic studies, it has been evaluated that ICE-1 and ICE-2 algorithms are suitable for inland water measurements as well (Lee et al., 2011). A demonstration of ICE-1 and ICE-2 for ENVISAT pass #81, compared with three available gauge data, is shown in Fig. 3a. In this figure, we notice the peak of water level in the wet season measured individually by two ENVISAT passes and three gauge records match pretty well during the period 2003-2005. The mismatches during dry season are caused by uneven bathymetry and isolated water storage between the gauge stations (Qi et al., 2009). We finally chose the best-fitted ICE-2 in this study, as its root-mean-square-error (RMSE) against the Long-Kou gauge data was slightly better than ICE-1 (0.47 m for ICE-2 and 0.48 m for ICE-1) during this 3-year validation.

The 8-day composite of MODIS surface spectral reflectance data (MOD09A1) at the 500 m spatial resolution provide seven bands of reflectance values with a viewing width of about 2,300 km. The fine, temporal (1-2 days) and spatial resolutions of MODIS/Terra data made it feasible to detect both short-term and small-scale geophysical variations.

The normalized difference water index (NDWI), computed from mixed band ratios, first introduced by McFeeters (1996), followed by the modified NDWI (MNDWI) that was further refined by Xu (2006) and Hui et al. (2008) to compute the Landsat Thematic Mapper (TM) images for water identification. The original form of MNDWI is based on the following expression:

$$MNDWI_{(Landsat)} = \frac{Green - NIR}{Green + NIR} \quad \text{(equation 1)}$$

where *Green* is the Landsat TM band 2 at 520-600 nm and *NIR* the near infrared, lower reflectance band 5 at 1550-1750 nm. We adopted the MNDWI according to Hui et al. (2008) but with a different selection of bands due to the improvement in MODIS multi-band ratio given by Westra and De Wulf (2009). The MNDWI for MODIS is computed as follows:

$$MNDWI_{(MODIS)} = \frac{Green - NIR}{Green + NIR} \quad \text{(equation 2)}$$

where *Green* is the MODIS 500 m high surface reflectance band 4 at 545-565 nm and *NIR* the near infrared, lower reflectance band 6 at 1628-1652 nm. The differentiated ratio of these two bands benefits from the different electromagnetic absorption by water molecules, enhancing image pixels with a weaker absorbance at wavelengths close to 500 nm. However, as the passive-microwave radiometry is a weather-dependent optical technique, cloud cover during the rainy season becomes an important issue that can cause certain image composites unusable.

We computed the MNDWI from MODIS spectral reflectance data as the horizontal delineation of water bodies. In addition, the ENVISAT radar altimeter waveform re-tracked height archived in the GDR was obtained as the vertical (water level) difference and water boundary evaluation. As shown by Chen and Lin (2004), snail habitats are strongly dependent on the physical structure of water/land boundaries and changes of the water surface. The greenery of the lakeshore marshlands indicates the general range of the snail drift outward with increased water levels, while MODIS and ENVISAT data complement each other when building a complete, continuous water surface profile over a time span.

MODIS MNDWI threshold evaluation

To determine the empirical MNDWI threshold at Poyang Lake and the surrounding floodplain, we overlaid ENVISAT altimetry points onto MNDWI at the

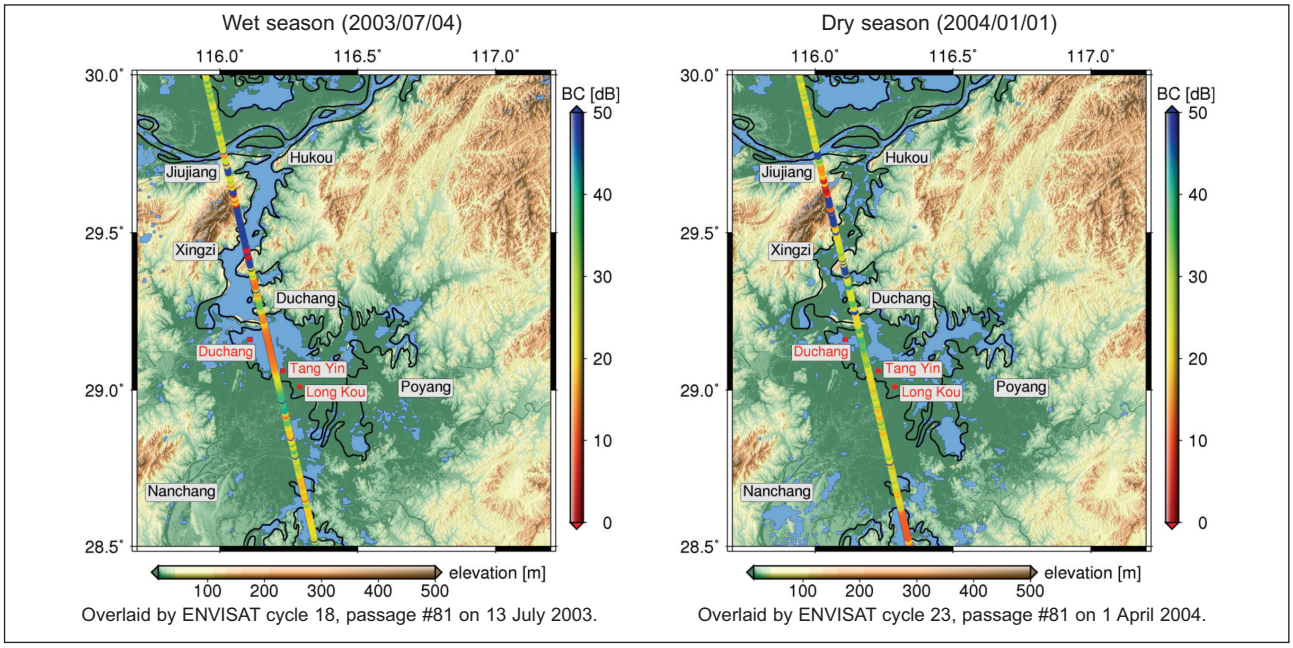

Fig. 4. The water surface of the Poyang Lake estimated by MODIS MNDWI and overlaid by ENVISAT tracks at two different seasons. Gauge data collected at three water-level gauges at Du-Chang, Tang-Yin and Long-Kou (red text). The ENVISAT ground track is colour-coded by backscatter coefficient (BC) implying surface roughness. The blue areas indicating water surface are the MNDWI (>0.1) values computed from individual MODIS surface reflectance data. The black contour indicates the average long-term lake/shore boundary similar to the lake surface as shown in Fig. 2.

time when two measurements were nearly coincident. As shown in Fig. 4, the Poyang Lake water storage in the wet season (left panel) and the dry (right panel) is quite different. In the wet season (mid-June to late October), MNDWI computed around 4 July 2003, shows that influx from the Yangtze River overflows part of the counties of Hukou and Jiujiang at the northern end of the lake. In the left panel of Fig. 4, the colour-coded line shows ENVISAT cycle 18, passage #81 (of 13 July 2003), which confirms that the water-covered area stretches between 29.05°-29.25° N and 29.33°-29.36° N since the back-scattering coefficients (BCs) imply consistently smoother (~15 dB) returns from the homogeneous water surface. In contrast, the right, dry-season panel shows a lower, dispersed water surface, while the upstream influx from Yangtze River is extremely reduced. The MNDWI, computed around 1 January 2004, shows the water coverage mainly in the eastern and southern parts of the lake. The ENVISAT altimetry points show that the specular reflection from mixed sediment and partial water surfaces leads to frequent BC oscillation, similar to so-called σ_0 bloom (Tournadre et al., 2006), with the only broader range of water detected at 28.5°-28.73° N. The empirical iteration comparing MNDWI with the ENVISAT BCs shows a MNDWI threshold of just above 0.1, as given in Fig. 4, is the optimum setting for this study region, just slightly higher than the figure (0.08) used by Westra and De Wulf (2009) and Jung et al. (2011). Fig. 4 also depicts that the three gauges available in this study are not homogeneously submerged into water all-year-round. Therefore, isolated gauge data are not reliable for synoptically monitoring of water dynamics over the whole area. A preferred way to watch the inundation area in multiple dimensions is to combine theses datasets in a synergistic scheme.

Validation of satellite observations

Time series of water level and water extent variation during 2000-2011 is shown in Fig. 3b. The water surface expansion computed by MNDWI (right ordinate) is comparable with the seasonal variation in the water level as measured by ENVISAT altimetry (left ordinate). It should be emphasised that MNDWI has a better temporal resolution (8-day) compared with altimetry data (30- or 35-day), which apparently poses greater fluctuation in the time series. This figure also illustrates an atypical Yangtze River flood during May to September in 2010. It is believed that this event was caused by melting snow, massive rainfalls and continuous discharge from the Three Gorges Dam upstream. Beside this anomaly, the end of this time series also matches well with the exceptional drought that the Yangtze River basin encountered in early summer 2011, while delay of the high-water season made the water level and surface remain in the channel and depressions throughout June.

Including the extraordinary peak, which occurred in 2010, and removing all seasonal sinusoidal signals, the 8-year linear trend of water level between November 2003 and June 2011 is negative for ENVISAT passage #81 at -0.03 m/year and positive for passage #490 at 0.01 m/year. In addition, the trend of shrinking water surface seen by MODIS from 2000 to mid-2011 was estimated at -33 km^2/year. The time series up to 2008 quantitatively agree with independent measurements reported by Uribe et al. (2009). It is assumed that decrease during the last decade was caused by several factors. Changes in regional climate would dominate the decreasing precipitation within the Yangtze River catchment area. In addition, the Three Gorges Dam, which is located ~700 km upstream from the Poyang Lake, began to impound water in 2003 and has been in full operation since 2008, also regulates water flows between seasons. Water dynamics changes caused by the dam lower the water level in the summer and shorten the dry season by a more continuous water flow.

Estimation of snail habitats

The geophysical requirement of snail habitats has been examined by Chen and Lin (2004) and Zhang et al. (2009), who considered distance to water-body, annual submergence rate, vegetation coverage and elevation above the mean, low-water level. A conceptual intersection of these constrains is demonstrated in Fig. 5. In this study, we calculated the area for two separated zones, mainly categorised by their distance to water bodies, to estimate the high potential (<1,500 m to the shoreline) and low potential area (1,500-18,000 m to the shoreline) of snail habitats. The detailed setting of the associated parameters is given in Table 1.

First, we re-sampled and linearly interpolated the 8-day MNDWI and 16-day EVI into a 4-day, 0.5 km grid map for the period of 2002-2010, for which the *in situ* investigation of the extent of the *Oncomelania* snail habitats in Jiangxi province is available. This information comes from the Ministry of Health (MoH) of P.R. China (http://www.moh.gov.cn). For the topographical reference of elevation, we adopted 3 arc-seconds (~100 m in spatial resolution) from the Shuttle Radar Topography Mission (SRTM) digital

Table 1. Parameters settings for snail habitat estimates in zones with high or low potential.

Zone	Distance to water body (m)	Annual submergence (day/year)	Elevation (m)	Vegetation coverage (%)	Annual accumulated submergence (days)
High potential	<1,500	90-240	14-17	>50	>30
Low potential	1,500-18,000		11.5-17.5	>50	>30

elevation model (DEM) version 2.1 (SRTM3) and smoothed the data into the cells of the map. In addition to the reported high-density zone (14-17 m in altitude) around the lake (Chen and Lin, 2004), we also referred to the actual variation of water level recorded by altimetry and *in situ* gauge data, indicating a low-potential habitat ranging from 11.5 to 17.5 m in altitude. Finally, pixels in the 0.25 km^2 grid that fulfil the parametric thresholds shown in Table 1 were classified as areas of either high or low potential.

Ahead of the model prediction, the annual submergence rate for each year was analysed and verified based on the reconstructed time series of MNDWI (an average of 2002-2010 shown as example in Fig. 6a). According to Chen and Lin (2004), most snails are found during the 90 to 240 days of annual submersion, which is equivalent to 25-65% of the year, while early flood or delayed recession of the lake water usually hinders snail propagation in this region. To examine this pattern, we conducted a spatio-temporal comparison between water extent and the snail habitat area. Fig. 6b reveals the average snail habitat hotspots for October, the normal annual peak, in the 2002-2010 period. To verify these hotspot estimates, based on the low-potential area setting, and the relation to the variation of the water surface, we delineated the submergence area for three parts of the year: May, July-August and October, which corresponds to the times before and after the flood season. While comparing the spatial distribution of the snail habitats (Fig. 6b) and seasonal water outlines, the relative position supports the hypothesis that the snail habitat in October tends to spread into the area submerged in summer, and matches well with the 25-65% interval seen in Fig. 6a.

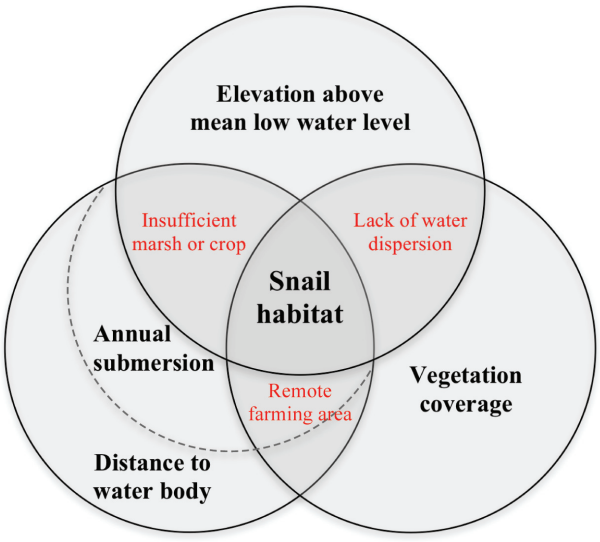

Fig. 5. Conceptual diagram showing the union (black) and partial union (red) area among the geophysical factors suitable for snail habitats.

Following the seasonal analysis, suitable snail habitat areas were examined from the spatial point of view during 2002-2010. A pixel-wise computation based on the average of data spanning the entire period was conducted to estimate the geolocation, i.e. where the occurrence of snail habitats tends to be higher. This averaged annual occurrence rate was computed by counting the number of years within the time span deemed suitable for snail habitats and then divide by the total number of years (9 in this case). Next, the snail habitat area predicted in 2008 by our model was compared with the prevalence observed in the field by Hu et al. (2013). Finally, the temporal variation of potential snail habitats over the entire basin was computed and compared with the MoH report.

Results

The spatial variation of suitable snail habitats, based on the 2002-2010 average and computed as explained above (under estimation of snail habitats), is displayed. In Fig. 7a, it can be seen that the extent (colour-coded by yellow-to-red dots) covers a large part of the lake basin and that it is highly correlated with the annual submergence rate at the 25-65% interval shown in Fig. 6a. In Fig. 7a, we note that the west-to-south part of the Poyang Lake basin is the preferable snail habitat area. In contrast, the higher undulation of terrain on the north side of the basin blocks possible transmission towards the hillside. It is also seen that a few spots along the main stream of the Yangtze River raise concerns about possible dis-

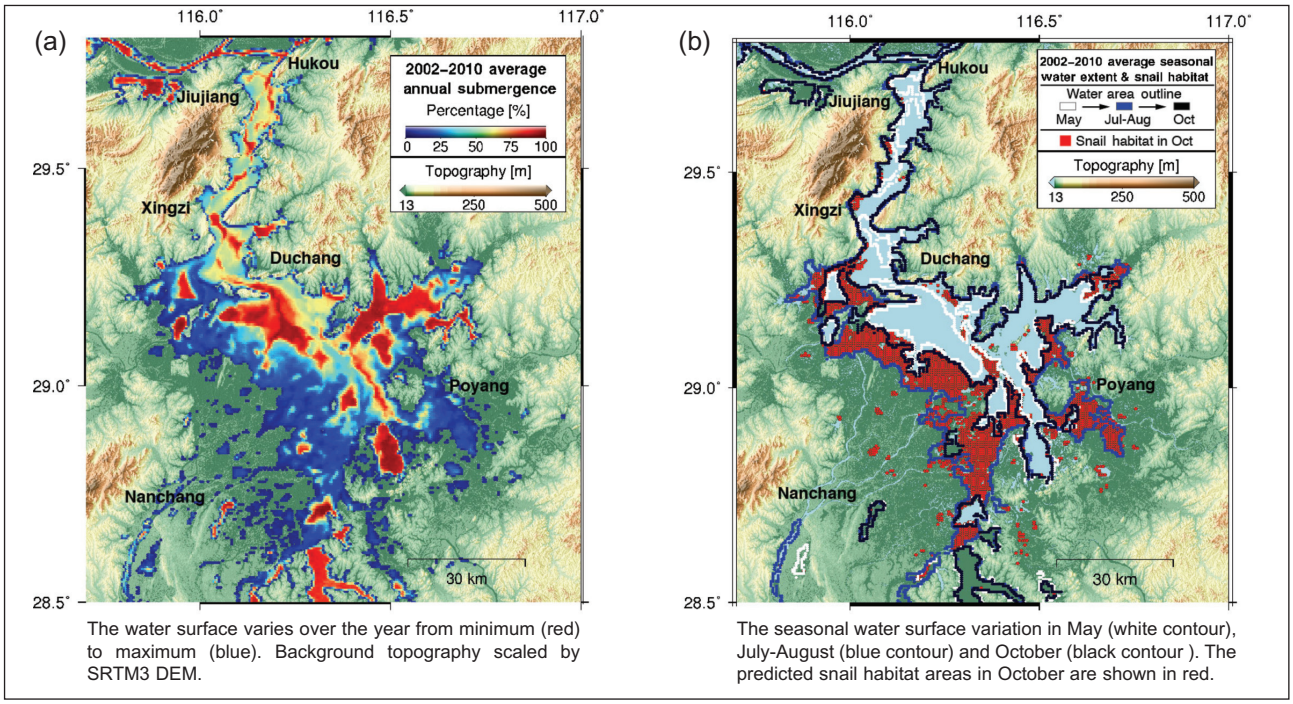

The water surface varies over the year from minimum (red) to maximum (blue). Background topography scaled by SRTM3 DEM.

The seasonal water surface variation in May (white contour), July-August (blue contour) and October (black contour). The predicted snail habitat areas in October are shown in red.

Fig. 6. The seasonal variation of the Poyang Lake surface estimated by MODIS MNDWI based on an average for 2002–2010 (a) with the October snail habitat hotspots overlaid (b).

ease dissemination. A blow-up view of the area near Xingzi county northwest of the Poyang basin (Fig. 7b) shows that the snail habitat occurrence at this location is higher than elsewhere due to the flat terrain and densely covered river channels. To verify this pattern, we isolated the 2008 estimate and compared it with the local survey of schistosomiasis prevalence in Xingzi county reported by Hu et al. (2013). In Fig. 8, the predicted snail habitats (red dots in left panel) in 2008 visually agree well with the

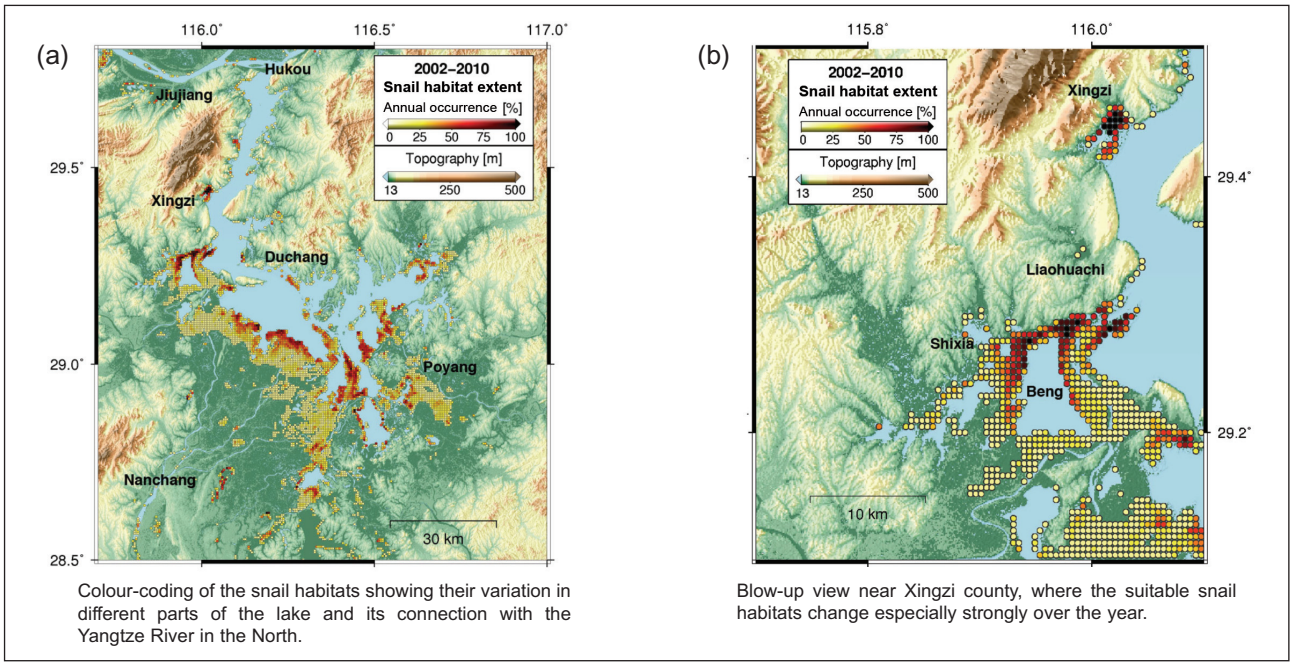

Colour-coding of the snail habitats showing their variation in different parts of the lake and its connection with the Yangtze River in the North.

Blow-up view near Xingzi county, where the suitable snail habitats change especially strongly over the year.

Fig. 7. Annual variation of snail habitats estimated by multiple environmental factors based on the period of 2002–2010. (a) Average occurrence of snail habitat extent over the entire basin. Color scale (yellow-to-red) indicates how many percent of days in a year is deemed suitable for *Oncomelania* snail to reside. (b) A blow-up view near Xingzi county, where the annual occurrence is higher over the lake basin and the *in situ* data is available in 2008.

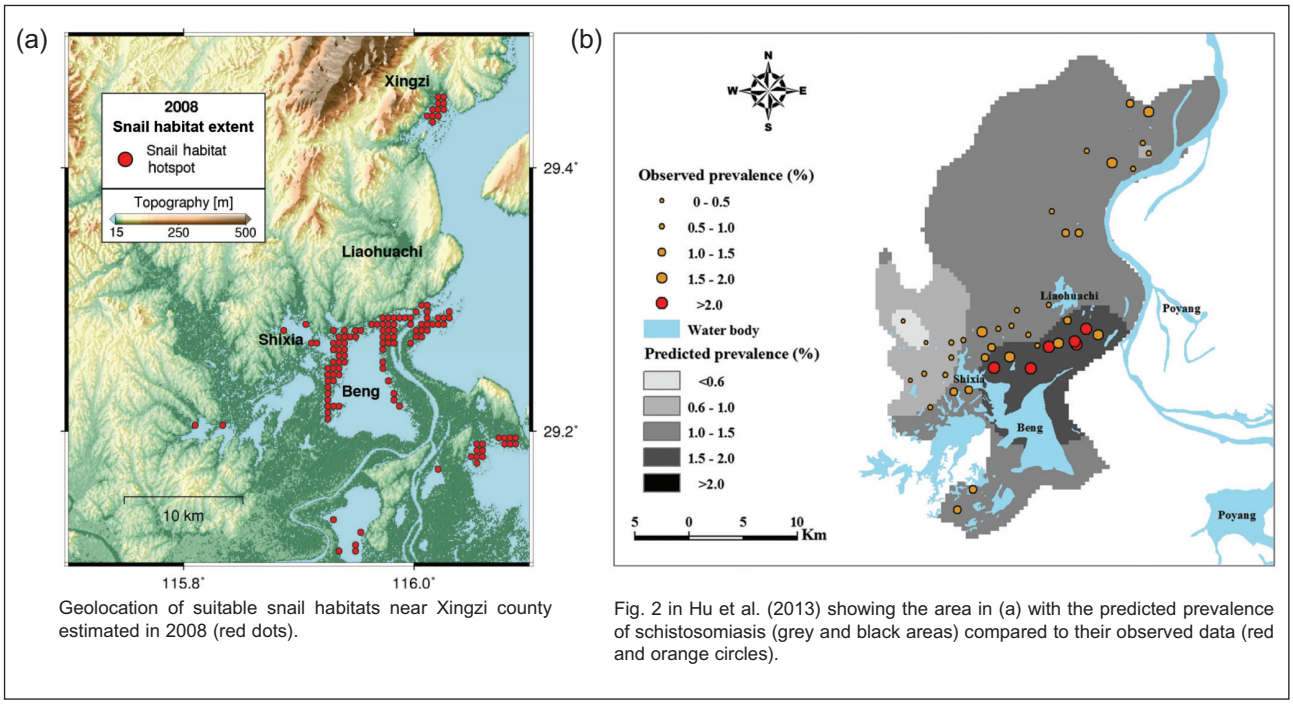

Geolocation of suitable snail habitats near Xingzi county estimated in 2008 (red dots).

Fig. 2 in Hu et al. (2013) showing the area in (a) with the predicted prevalence of schistosomiasis (grey and black areas) compared to their observed data (red and orange circles).

Fig. 8. Snail habitats estimated by multiple environmental factors based on the year of 2008 (a) compared field observations (b).

actual prevalence surrounding Beng Lake, Shixia and near Xingzi city.

A temporal comparison between our estimate and the official MoH report of the extent of *Oncomelania* snail habitats is given in Fig. 9. As depicted, the low-potential estimates encompassing a broader range in space matches fairly well in tendency with reported data in 2002-2006 and 2009-2010. The double-peak pattern in a year also agrees with the snail seasonal life cycle described in Chen and Lin (2004). High-potential area estimates, although overall have a discernible bias toward MoH reported areas, are basically correlated with low-potential estimates in time, characterising the extent of hotspots that varies annually between 20 and 240 km^2. However, an opposite trend between low-potential estimates and MoH in 2007 and 2008 is noted. In addition, two overestimates in 2002 and 2007, as well as notable underestimates in 2006, 2008 and 2009 are also observed. We suspect that these mismatches are possibly subject to other constraints missing in the model, such as intervention by local agencies, dyke construction, higher altitude habitat, etc.

The statistical comparison of the estimated extent between the satellite-borne data and the MoH report for *Oncomelania* snails in Jiangxi province is given in Table 2. The satellite-borne estimate here is the annual peak in the time series that approximates the maximum extent in a year. In Table 2, a good correlation between high-potential estimate and *in situ* data is seen with the Pearson's r = 0.82, whereas the low-potential estimate has a relatively poor correlation at just 0.69. The contribution of the low-potential estimate is a better quantification of the total extent at a RMSE of 94 km^2 and a smaller bias at 33 km^2 compared with the *in situ* data. Therefore, a combination of both high and low potential estimates provides a complete evaluation of variation of snail's habitat both spatially and temporally.

Table 2. Comparison between two satellite-estimated zones and the MoH-reported extent of *Oncomelania* snail habitats in Jiangxi province.

Zone	Pearson's r	RMSE* habitat extent estimate (km^2)	Habitat extent estimate bias (km^2)
High potential	0.82	N/A**	180
Low potential	0.69	94	33

*Root-mean-square-error; **estimates too low.

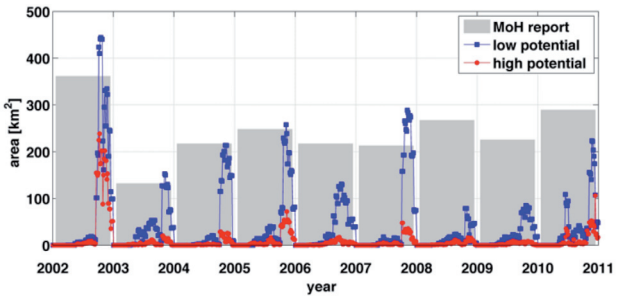

Fig. 9. *Oncomelania* snail habitat areas in Jiangxi province by different estimates. The red and blue lines represent the high and low potential models, respectively. The grey bars indicate the results of in situ investigations in the province.

Discussion

The transmission of parasitic diseases relies on various factors, in particular bioclimatic variables that facilitate the propagation of intermediate hosts and vectors. The delineation of areas endemic for schistosomiasis is strongly associated with humidity and water bodies (Lleo et al., 2008). Spatial characterisation is thus applicable in light of the fact that this disease is regularly enclosed in regional and temporal windows leading us to use remote sensing and geodetic measurements to indicate and monitor proxies such as presence of its intermediate host *O. hupensis*. Specifically, we have estimated possible, endemic regions by focusing on the potential for habitat in the Poyang Lake, a region in P.R. China endemic for schistosomiasis. It is anticipated that the technique developed herein can be further extended to other infectious diseases transmitted under similar mechanism and in other parts of the world.

How to reduce mortality and morbidity rates due to schistosomiasis among residents in the endemic areas of the world depends mainly on improvement of public hygiene, chemotherapy and the potential addition of vaccines (Siddiqui et al., 2011). However, control activities has started to shift its focus from morbidity to transmission and the latter is rapidly becoming a critical task for many tropical countries, which requires well-established systems for monitoring surrounding environmental factors. The mapping of areas potentially at risk for schistosomiasis transmission through association with water dynamics provides an important way of assisting public health agencies in the fields of surveillance and intervention. In this study, a fairly good inter-annual variation of the extent of *Oncomelania* snail habitats was observed from satellite data. However, small-scale factors such as dyke construction, intervention measures, and human activities are difficult to observe by satellite imaging. These factors can therefore introduce errors in estimates of areas at potential risk and satellite surveys therefore be seen as a complement to Earth-bound observations in refining the predictive model presented here. Additionally, by exclusively using a remote-sensing strategy we may encounter limitations in classifying agricultural types that are hospitable for specific *Oncomelania* snails, particularly since these snails mostly dwell in just few types of marshland. Therefore, current monitoring of large-scale vegetation by focussing on high-biomass regions could be subject to errors in snail habitat estimates. Another concern of multi-spectral analysis using low-cost and open-access satellite imagery is the currently available coarse spatial resolution (generally >30 m) that limits the capability of identification (Herbreteau et al., 2007). Nevertheless, the multivariate simulation developed in this study must be considered a useful, first step of a broad-range monitoring system for control and analysis of endemic areas.

Conclusions

Space-borne capability to measure water levels, inundation proliferation and environmental factors are accurate and complement *in situ* data. The spread of snail habitats can be used as proxy for disease transmission, even if the actual status of asymptomatic carriers, either human or snails, remains elusive. The prospect of using integrated altimetry and remotely sensed data is a useful strategy not only for surveying schistosomiasis risk but potentially also for monitoring other epidemics transmitted by similar water-associated vectors.

Under the present climate change scenario, the spatio-temporal (latitudinal, altitudinal and temporal) distributions of global infectious diseases are starting to become reshuffled (Lafferty, 2009) on the basis of changing geographical suitability, in particular for parasites as they are completely dependent on intermediate hosts and vectors. Significant fluctuations in atmospheric variables such as humidity, precipitation, and temperature biologically affect the population and activity of vectors living in the aquatic environment. Damming projects are on the increase under the forthcoming water-resource crisis and will probably accelerate the spread of diseases from rural endemic to urban regions, while changes in human population and residential areas pose an uncertainty in estimating prevalence and incidence of infectious diseases among economically emerging areas.

Parametric models linking geophysical and epidemiological dimensions are imperative to facilitate near-real time monitoring and early warning systems for the spread of infectious diseases. The successful demonstration of a predictive model for the Poyang Lake would be greatly beneficial for other endemic areas where *in situ* surveys are constrained. However, future studies to operate this model in forecast mode require the incorporation of geophysical variables such as accumulated rainfall and snowfall within the upstream catchment area of the Yangtze River.

Acknowledgements

The Ohio State University (OSU) component of this research was supported by grants by Environmental Protection Agency (grant no. RD-83519201), OSU's Climate, Water and Carbon (CWC) Program, and by the Chinese Academy of Sciences/SAFEA International Partnership Program for Creative Research Teams (grant no. KZZD-EW-TZ-05). We thank the editor-in-chief, Dr. Robert Bergquist, and anonymous reviewers for their constructive comments.

References

Alsdorf DE, Rodriguez E, Lettenmaier DP, 2007. Measuring surface water from space. Rev Geophys 45, 24.

Brown GS, 1977. The average impulse-response of a rough surface and its applications. IEEE Trans Antennas Propag 25, 67-74.

Uribe C, Li J, Daillet S, Chen X, Bergé-Nguyen M, Li J, Crétaux Jean-F, Huber C, Lai X, Marie T et al., 2009. Monitoring of the largest Chinese inland lakes within the ESA-MOST DRAGON project using conjointly ENVISAT image time series and altimetric data: case of Dongting and Poyang lakes. 13th World Lake Conference, 1-5 November 2009, Wuhan, China.

Chen HG, Lin DD, 2004. The prevalence and control of schistosomiasis in Poyang Lake region, China. Parasitol Int 53, 115-125.

Chen MG, 2014. Assessment of morbidity due to *Schistosoma japonicum* infection in China. Infect Dis Poverty 3, 6.

Chen X, Wu X, Wang L, Dang H, Wang Q, Zheng J, Guo J, Jiang Q, Zhao G, Zhou X, 2003. Schistosomiasis situation in the People's Republic of China in 2002. Chin J Schisto Cont 15, 241-244.

Chu YH, Li JC, Jiang WP, Zou XC, Fan CB, Xu XY, Dadzie I, 2008. Monitoring level fluctuations of the lakes in the Yangtze River basin from radar altimetry. Terr Atmos Ocean Sci 19, 63-70.

Davis CH, 1997. A robust threshold retracking algorithm for measuring ice-sheet surface elevation change from satellite radar altimeters. IEEE Trans Geosci Remote Sens 35, 974-979.

Davis GM, Wu WP, Liu HY, Williams GA, Lu SB, Chen HG, Seto E, 2002. Applying GIS and remote sensing to the epidemiology of schistosomiasis in Poyang Lake, Jiangxi Province, Ann GIS 8, 67-77.

Duan Y, Steil S, 2003. China three gorges project resettlement: policy, planning and implementation. J Refug Stud 16, 422-443.

Fu LL, Cazenave A, 2001. Satellite altimetry and Earth sciences, a handbook of techniques and applications, San Diego: Academic Press, International Geophysics Series, 69.

Herbreteau V, Salem G, Souris M, Hugot JP, Gonzalez JP, 2007. Thirty years of use and improvement of remote sensing, applied to epidemiology: from early promises to lasting frustration. Health Place 13, 400-403.

Hu CM, Chen ZQ, Clayton TD, Swarzenski P, Brock JC, Muller-Karger FE, 2004. Assessment of estuarine water-quality indicators using MODIS medium-resolution bands: initial results from Tampa Bay, FL. Remote Sens Environ 93, 423-441.

Hu Y, Zhang Z, Chen Y, Wang Z, Gao J, Tao B, Jiang QL, Jiang QW, 2013. Spatial pattern of schistosomiasis in Xingzi, Jiangxi province, China: the effects of environmental factors. Parasit Vectors 6, 214.

Hui FM, Xu B, Huang HB, Yu Q, Gong P, 2008. Modelling spatial-temporal change of Poyang Lake using multitemporal Landsat imagery. Int J Remote Sens 29, 5767-5784.

Jung HC, Alsdorf D, Moritz M, Lee H, Vassolo S, 2011. Analysis of the relationship between flooding area and water height in the Logone floodplain. Phys Chem Earth 36, 232-240.

Kim JW, Lu Z, Lee H, Shum CK, Swarzenski CM, Doyle TW, Baek SH, 2009. Integrated analysis of PALSAR/Radarsat-1 InSAR and ENVISAT altimeter data for mapping of absolute water level changes in Louisiana wetlands. Remote Sens Environ 113, 2356-2365.

Lafferty KD, 2009. The ecology of climate change and infectious diseases. Ecology 90, 888-900.

Lee H, Shum CK, Emery W, Calmant S, Deng XL, Kuo CY, Roesler C, Yi YC, 2010. Validation of Jason-2 altimeter data by waveform retracking over California coastal ocean. Mar Geod 33, 304-316.

Lee H, Shum CK, Tseng KH, Guo JY, Kuo CY, 2011. Present-day lake level variation from ENVISAT altimetry over the northeastern Qinghai-Tibetan Plateau: links with precipitation and temperature. Terr Atmos Ocean Sci 22, 169-175.

Lee H, Shum C, Tseng KH, Huang Z, Sohn HG, 2013. Elevation changes of Bering Glacier system, Alaska, from 1992-2010, observed by satellite radar altimetry. Remote Sens Environ 132, 40-48.

Lei ZL, Zheng H, Zhang LJ, Zhu R, Guo JG, Li SZ, Wang LY, Chen Z, Zhou XN, 2011. Schistosomiasis status in People's Republic of China in 2010. Chin J Schisto Control 23, 599-604.

Li YS, Raso G, Zhao Y, He HK, Ellis M, McManus DP, 2007. Large water management projects on schistosomiasis transmission and control in the Dongting Lake region, China. Emerg Infect Dis 13, 973-979.

Liang S, Seto EYW, Remais JV, Zhong B, Yang CH, Hubbard A, Davis GM, Gu XG, Qiu DC, Spear RC, 2007. Environmental effects on parasitic disease transmission exemplified by schistosomiasis in western China. Proc Natl Acad Sci U.S.A. 104, 7110-7115.

Liu Q, 2006. Monitoring area variation and sedimentation patterns in Poyang Lake, China using MODIS medium-resolution bands. ITC 47. International Institute For Geo-Information Science And Earth Observation, Enschede, The Netherlands.

Lleo MM, Lafaye M, Guell A, 2008. Application of space technologies to the surveillance and modelling of waterborne diseases. Curr Opin Biotechnol 19, 307-312.

Lu Z, Kim JW, Lee H, Shum CK, Duan JB, Ibaraki M, Akyilmaz O, Read CH, 2009. Helmand river hydrologic studies using ALOS PALSAR InSAR and ENVISAT altimetry. Mar Geod 32, 320-333.

McFeeters SK, 1996. The use of the normalized difference water index (NDWI) in the delineation of open water features. Int J Remote Sens 17, 1425-1432.

McManus DP, Gray DJ, Li YS, Feng Z, Williams GM, Stewart D, Rey-Ladino J, Ross AG, 2010. Schistosomiasis in the People's Republic of China: the era of the Three Gorges Dam. Clin Microbiol Rev 23, 442-466.

Peng WX, Tao B, Clements A, Jiang QL, Zhang ZJ, Zhou YB, Jiang QW, 2010. Identifying high-risk areas of schistosomiasis and associated risk factors in the Poyang Lake region, China. Parasitology 137, 1099-1107.

Qi SH, Brown DG, Tian Q, Jiang LG, Zhao TT, Bergen KA, 2009. Inundation extent and flood frequency mapping using Landsat imagery and digital elevation models. Gisci Remote Sens 46, 101-127.

Ross AG, Li Y, Williams GM, Jiang Z, McManus DP, 2001. Dam worms. Biologist 48, 121-124.

Siddiqui AA, Siddiqui BA, and Ganley-Leal L, 2011. Schistosomiasis vaccines. Hum Vaccin 7, 1192-1197.

Spear RC, Hubbard A, Liang S, Seto E, 2002. Disease transmission models for public health decision making: toward an approach for designing intervention strategies for schistosomiasis japonica. Environ Health Perspect 110, 907-915.

Spear RC, Seto E, Liang S, Birkner M, Hubbard A, Qiu D, Yang C, Zhong B, Xu F, Gu X et al., 2004. Factors influencing the transmission of *Schistosoma japonicum* in the mountains of Sichuan province of China. Am J Trop Med Hyg 70, 48-56.

Tournadre J, Chapron B, Reul N, Vandemark DC, 2006. A satellite altimeter model for ocean slick detection. J Geophys Res Oceans 111, 13.

Tseng KH, Shum CK, Lee H, Duan J, Kuo CY, 2011. Satellite observed environmental changes over the Qinghai-Tibetan Plateau. Terr Atmos Ocean Sci 22, 229-239.

Tseng KH, Shum CK, Yi Y, Emery WJ, Kuo C, Lee H, Wang H, 2014. The improved retrieval of coastal sea surface height by retracking modified radar altimetry waveforms. IEEE Trans Geosci Remote Sens 52, 991-1001.

Tseng KH, Shum CK, Yi Y, Lee H, Cheng X, Wang X, 2013. ENVISAT altimetry radar waveform retracking of quasi-specular echoes over ice-covered Qinghai Lake. Terr Atmos Ocean Sci 24, 615-627.

Utroska JA, Chen MG, Dixon H, Yoon S, Helling-Borda M, Hogerzeil HV, Mott KE, 1989. An estimate of global needs for praziquantel within schistosomiasis control programmes. Geneva: World Health Organization, 92 pp.

Utzinger J, Zhou XN, Chen MG, Bergquist R, 2005. Conquering schistosomiasis in China: the long march. Acta Trop 96, 69-96.

Wang Q, Zhang ZX, Mu FY, Yi L, Wang J, 2007. Research on "Beijing 1" micro-satellite image quality and land use classification precision. J China Univ Min Technol 36, 3, 386.

Wessel PP, Smith WHF, 2010. The generic mapping tools, version 4.5.2. Technical Reference and Cookbook.

Westra T, De Wulf RR, 2009. Modelling yearly flooding extent of the Waza-Logone floodplain in northern Cameroon based on MODIS and rainfall data. Int J Remote Sens 30, 5527-5548.

Wu ZD, Lu ZY, Yu XB, 2005. Development of a vaccine against *Schistosoma japonicum* in China: a review. Acta Trop 96, 106-116.

Xu HQ, 2006. Modification of normalised difference water index (NDWI) to enhance open water features in remotely sensed imagery. Int J Remote Sens 27, 3025-3033.

Zhang MM, Lee HK, Shum CK, Alsdorf D, Schwartz F, Tseng KH, Yi Y, Kuo CY, Tseng HZ, Braun A et al., 2010. Application of retracked satellite altimetry for inland hydrologic studies. Int J Remote Sens, 31, 3913-3929.

Zhang ZJ, Carpenter TE, Lynn HS, Chen Y, Bivand R, Clark AB, Hui FM, Peng WX, Zhou YB, Zhao GM et al., 2009. Location of active transmission sites of *Schistosoma japonicum* in lake and marshland regions in China. Parasitology, 136, 737-746.

Zheng H, Zhang LJ, Zhu R, Xu J, Li SZ, Guo JG, Xiao N, Zhou XN, 2011. Schistosomiasis situation in the People's Republic of China in 2011. Chin J Schisto Contr 24, 621-626 (in Chinese).

Zhou XN, Guo JG, Wu XH, Jiang QW, Zheng J, Dang H, Wang XH, Xu J, Zhu HQ, Wu GL et al., 2007. Epidemiology of schistosomiasis in the People's Republic of China, 2004. Emerg Infect Dis 13, 1470-1476.

Zhou XN, Wang LY, Chen MG, Wu XH, Jiang QW, Chen XY, Zheng J, Utzinger J, 2005. The public health significance and control of schistosomiasis in China - then and now. Acta Trop 96, 97-105.